Cement and Concrete Research 40 (2010) 226–234

Contents lists available at ScienceDirect

Cement and Concrete Research

journal homepage: http://ees.elsevier.com/CEMCON/default.asp

Rheology of fiber reinforced cementitious materials: classification and prediction

Laetitia Martinie, Pierre Rossi, Nicolas Roussel *

Université Paris Est, Laboratoire Central des Ponts et Chaussées, Paris, France

ARTICLE INFO

Article history:
Received 25 February 2009
Accepted 25 August 2009

Keywords:
Rheology (A)
Mixture proportioning (A)
Fresh concrete (A)
Aggregate (D)
Fiber reinforcement (E)

ABSTRACT

In this paper, the effect of rigid straight fibers on the yield stress of cementitious materials is studied. A simple model describing the contact network between rigid fibers inside the material is first derived from the physical phenomena involved in the case of spherical inclusions. As soon as this contact network becomes percolated, the yield stress of the mixture increases by several orders of magnitude. A prediction of the critical fiber amount leading to a very strong increase of the yield stress of any cement paste, mortar or concrete is then derived. A simple and helpful mix design criterion for Ultra High Performance Fiber Reinforced Concretes is finally proposed and applied to several mix proportions from literature.

1. Introduction

Fibers in cementitious materials have a very positive influence on the mechanical properties of the material in its hardened state (tensile strength and ductility [1–5]). This influence strongly depends on the aspect ratio r of the fiber, namely the ratio between the length l and the diameter d of the fiber and on the concentration of fibers. Most results in literature show that mechanical performances of the material increase with both the aspect ratio and the concentration of the fibers. This topic has been the subject of numerous papers focusing on the physical and mechanical phenomena involved in the cracking and pulling out of fibers in a cementitious matrix according to their shape, volume fraction and orientation [6–16].

The literature in the case of fresh properties of cementitious materials containing fibers is not as abundant, but it has been shown that addition of fibers decreases the workability of the material. This effect increases with the volume fraction and aspect ratio of the fibers [2,4,5,17]. Hughes and Fattuhi [17] observed that, although slump is not always a suitable test to measure the fluidity of a fiber reinforced material [18], it decreases when the product $r\sqrt{\phi_f}$ increases, with ϕ_f the fiber volume fraction. Other researchers [2–4,19–22] observed in a similar way that slump decreases when the product $r\phi_f$ defined as the *fiber factor*, increases. Grünewald and Walraven [3], Bui et al. [23], Ding et al. [24], Ferrrara et al. [25] and Banfill et al. [26] measured, instead of a decrease of the slump or slump flow, an increase of the yield stress of the material using concrete rheometers. This result was expected knowing the correlation existing between slump (or slump flow) and yield stress [27–29].

Swamy and Mangat [30] showed the existence of a critical concentration of fibers above which the concrete could not flow anymore, even when the fibers were added to very fluid concretes such as Self Compacting Concretes. Above this concentration, it was observed that fibers tend to form *clumps* or *balls*. Keeping in mind that the mechanical properties in the hardened state increase with the fiber amount, this critical concentration is therefore defined by many authors as an optimum content of fiber in the literature. This represents a compromise between mechanical properties in the hardened state and fluidity in the fresh state. Most results tend to indicate that this critical volume fraction decreases with increases in the coarse particle volume fraction in the mixture. It also decreases when the aspect ratio of the fibers increases [17,26]. The values of the fiber factor, $r\phi_f$ when this critical concentration is reached cited in the literature are between 0.2 and 2 depending on the other components in the materials tested [2,26,31,32].

Contrary to spherical rigid inclusions, in the case of rigid fibers, the flow can induce a preferred orientation of the fibers which modifies the material fresh properties and, after setting, strongly influences the mechanical properties of the resulting fiber-reinforced composite [8,31–34]. However, in this paper, we will use results obtained either from tests, in which the flow was too short for this orientation to affect the behavior of the material or from tests, in which there was no steady streamlines allowing for this orientation to appear. We will therefore focus here on the isotropic rheological behavior of fresh fiber reinforced cementitious materials.

It was shown in [6] that workability could be generally considered as independent of the fiber type but that crimped fibers could lead to slightly lower workability. We will not deal here with the effect of specific shapes on the rheological properties of the fresh material.

In this paper, we first derive from the physical phenomena involved in the formation of a contact network between simple spherical inclusions a simple model describing the contact network between

* Corresponding author.
E-mail address: Nicolas.roussel@lcpc.fr (N. Roussel).

0008-8846/$ – see front matter
doi:10.1016/j.cemconres.2009.08.032

rigid fibers inside the material. We then propose a criterion allowing for the distinction between rigid and flexible fibers. We show that a prediction of the critical fiber amount leading to a very strong increase of the yield stress of a cement paste, mortar or concrete can be derived from the proposed approach. A mix design criterion is finally proposed and applied to several mix proportions from the literature.

2. Influence of the addition of rigid inclusions on the yield stress of concrete

Concrete components range from micrometer sized cement particles to centimeter sized aggregate particles and, in the study of the relation between mix design and rheological properties, multi-scale approaches seem very promising [35–37]. The simplest multi-scale approach only involves two scales and it is therefore often considered that concrete is a suspension of aggregate particles (sand and gravel) in a suspending fluid (cement paste). It can then be expected, as a first approximation, that, as for many suspensions in nature or industry, the yield stress of the suspension (*i.e.* the concrete) is proportional to the yield stress of its suspending fluid (*i.e.* the constitutive cement paste).

This statement can be extrapolated from general relations similar to the Krieger–Dougherty relation for apparent viscosity [38–40], which relate the rheological properties of the suspending fluid and the volume fraction ϕ of the particles to the rheological properties of the mixture. The general form of these relations is:

$$\tau_0^{conc} \approx \tau_0^{cp} f(\phi / \phi_m) \quad (1)$$

where τ_0^{conc} and τ_0^{cp} are respectively the yield stress of the concrete and of the cement paste. ϕ_m is the dense packing volume fraction (Cf. Fig. 1(c)). We will make here a distinction between the dense packing volume fraction ϕ_m and the maximum packing fraction ϕ_M, which can only be reached by bringing to the system an infinite amount of energy. In the case of spheres for example, the dense packing fraction ϕ_m is around 0.64 (see Fig. 1(c)) whereas the maximum packing fraction ϕ_M is equal to 0.74.

It must not be forgotten that phenomenological relations such as Eq. (1) (whether dealing with yield stress or viscosity) have been historically established for semi-dilute systems and therefore purely hydrodynamic interactions between the suspending fluid and the particles [38] and, although they are able, from an experimental point of view, to describe the divergence of the viscosity close to the dense packing fraction, they should, from a theoretical point of view, apply only for moderate volume fraction of inclusions.

It is of great interest to study the relative yield stress of the concrete (*i.e.* the ratio between the yield stress of the concrete and the yield stress of the cement paste) as it allows theoretically to focus on the effect of the granular inclusion content (*i.e.* $f(\phi/\phi_\mathrm{m})$) independently of the cement paste mix design. The study of the variations of the relative yield stress is therefore the study of the rigid inclusion interactions. When rigid particles such as sand and gravel particles are mixed in a fluid such as cement paste, the type of particle/particle or fluid/particle interactions may vary according to the packing of the particles in the system.

At low volume fractions, the system can be considered as semi-dilute (Fig. 1(a)) and the particle interactions are hydrodynamic: the motion of particles such as sand grains or gravel in a cement paste implies some flow or deformation of the cement paste, which itself can affect the flow velocities or displacement of other particles. If the concrete is flowing, some analogous effect occurs that induces additional energy dissipations so that the apparent viscosity of the cement paste plus the grains is greater than that of the cement paste alone. Thus the apparent viscosity of a concrete increases with the volume fraction of inclusions. It can be noted here that, in the case of the asymptotic case of an ideal dilute system, there would not be any interactions between the particles at all through hydrodynamic effects, the particles being far enough one from one another to stay undisturbed by the relative motions of other particles. Most relations described above linking the properties of the mixture to the properties of the suspending fluid are only valid in the dilute and semi-dilute regimes.

At higher volume fractions, direct contacts may occur between aggregate particles. The predominance of contacts in the physical behavior necessarily results from the existence of a considerable amount of contacts throughout the suspension, so that we conclude that this situation can be associated with the existence of a continuous network of particles in contact (Fig. 1(b)). Since this phenomenon is associated with a percolation process, it occurs when the solid fraction is larger than a critical one (ϕ_c), called random loose packing. Current knowledge in this field does not make it possible to predict theoretically the value of ϕ_c in the case of spherical rigid particles. However, experimental and numerical results indicate that, for uniform spheres ($\phi_\mathrm{m} = 0.64$), ϕ_c should be around 0.5 [41]. However, ϕ_c should increase in the case of poly-disperse particles such as sand or gravel as the average distance between particle scales with $(\phi/\phi_\mathrm{m})^{-1/3}$ (which is expected to correlate to the average number of contacts between particles) and therefore increases when ϕ_m increases. It may thus be of interest to deal with the value of the relative solid volume fraction (ϕ/ϕ_m) that can be compared to the critical value deduced from the mono-sized sphere case $\phi_\mathrm{c}/\phi_\mathrm{m} \cong 0.8$ instead of dealing with the value of the volume fraction itself.

This simple concept was applied to experimental measurements of the yield stress of widely varying concretes in [37]. It was shown that it is indeed around the transition value $\phi_\mathrm{c}/\phi_\mathrm{m} \cong 0.8$ that a variation of several orders of magnitude of the yield stress of the tested concretes

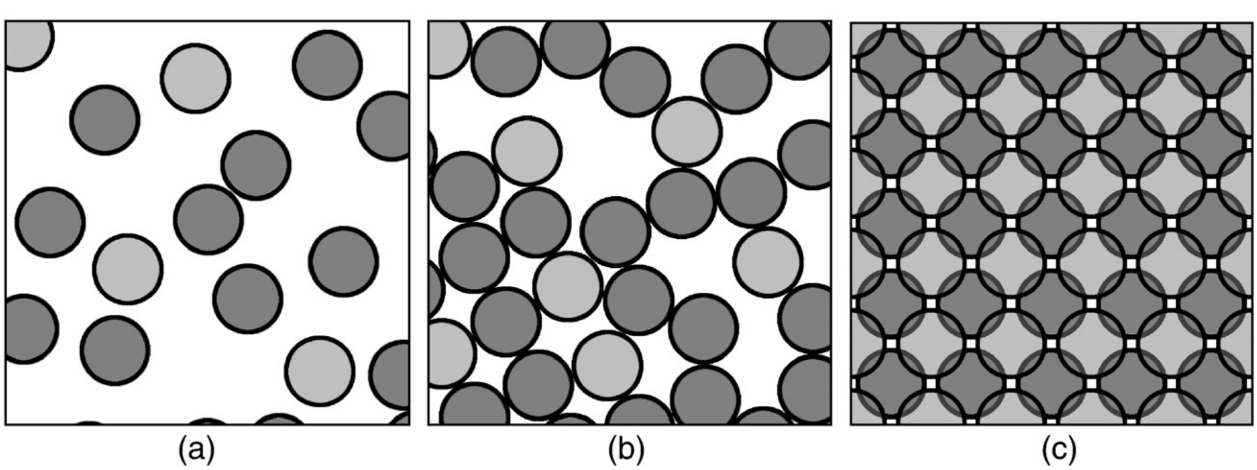

Fig. 1. Packing regimes in the case of spherical rigid inclusions. (a) Semi-dilute regime; (b) random loose packing; (c) dense packing.

occurs. This means that, below this transition value (*i.e.* below the random loose packing fraction), more or less direct contacts between the inclusions in this semi-dilute system can be neglected. This domain is the one where Self Compacting Concretes (SCC) may be mix-designed. It is moreover possible in this domain to predict the yield stress of the mixture using simple relation such as the one proposed in [40]. Inversely, above this transition value (*i.e.* above the Random Loose Packing), direct frictional contacts between particles start to dominate the rheological behavior of this dense system. Their highly dissipative nature strongly increases the yield stress of the concrete, turning any concrete into an Ordinary Rheology Concrete (ORC). In this regime, the behavior of the concrete does not depend much on the behavior of the cement paste but mainly on the volume fraction and on the dense packing fraction of the granular skeleton.

It has to be noted that the drastic reduction in the contribution of direct contacts between rigid particles around the transition cannot turn alone any ORC into a SCC. Indeed, the fact that the granular content is below the transition between semi-dilute and dense regimes only guarantees that the contribution of the coarse aggregates to the yield stress of the mixture will be low. In order to obtain a fluid concrete, one has to design a fluid cement paste. It has to be kept in mind that the yield stress of concrete will never be lower than the yield stress of its constitutive cement paste as adding aggregates to the mixture can only concentrate the deformation and deformation rate in the cement paste and therefore increase the capacity of the system to dissipate energy at a given macroscopic shear strain or shear rate. It has also to be kept in mind that, in the semi-dilute regime, the yield stress of the concrete is more or less proportional to the yield stress of the cement paste (see Eq. (1)). As a consequence, in order to mix design SCC, one has to ensure that the aggregate volume fraction is lower that the transition value and, moreover, that the yield stress of the cement paste is low (but sufficient to ensure the stability of the coarsest particles [42]).

In the following, we will extrapolate the same simple concept to cementitious materials containing fibers.

3. Distinction between rigid and flexible fibers

We will show in this paper that, as in the above case of rigid (almost) spherical inclusions, the strong decrease in fluidity of fresh composite cementitious materials find its origin in a direct contact network between fibers occurring at a critical volume fraction of fibers. This network can withstand an external load and therefore increase the yield stress of the considered material only if it consists of direct contacts between rigid bodies. It is therefore necessary to establish a distinct boundary between rigid and flexible fibers.

Different types of fibers are used in industry to reinforce cementitious materials. Some of them such as polypropylene (PP) or organic fibers are flexible whereas many rigid fibers, mostly steel fibers, are often used in civil engineering. It is however rather delicate to distinguish between rigid and non-rigid fibers. For example, although the Young modulus of carbon is almost the same as the Young modulus of steel, most high aspect ratio carbon fibers are not rigid because of their elongated shape. Moreover, although a fiber seems rigid in air or water, it may not be considered as rigid when sunk into a concentrated highly viscous cementitious suspension. A suitable criterion enabling the distinction between rigid and non rigid fibers should thus take into account the Young modulus of the fiber material, the shape of the fiber itself and the consistency of the cementitious material in which it is mixed.

We propose here to consider a fiber in a cementitious material as a beam uniformly loaded and to estimate the ratio of the deflexion of the fiber due to the fluid to the length of the fiber. This ratio should be negligible in the case of a rigid fiber (*e.g.* lower than 1%).

We first assume that the uniform load (in N/m) to which the fiber (*i.e.* the beam) is submitted is of order $\tau_0 d$, where τ_0 is the yield stress of the cementitious material in which fibers are added and d is the diameter of the fibers. The exact drag force exerted by the cementitious material on the fiber could of course be calculated but, as a first approach of the problem, we only consider here orders of magnitude. The order of magnitude of the deflexion f of the fiber is therefore:

$$f \cong \frac{\tau_0 d l^4}{EI} \tag{2}$$

where E is the Young modulus of the fiber material and I is of order d^4. Finally, the ratio between the deflexion and the length of the fiber is of order:

$$\frac{f}{l} \cong \frac{\tau_0}{E} r^3 \tag{3}$$

As an example, this ratio is of order 0.03% in the case of standard steel fibers (aspect ratio $r = 50$, Young modulus $= 210{,}000$ MPa) sunk into a SCC (yield stress $= 50$ Pa) whereas it is of order 66% when long carbon fibers (aspect ratio $r = 500$, Young modulus $= 190000$ MPa) are sunk into an ORC (yield stress $= 1000$ Pa). It can therefore be concluded that, although the Young modulus of carbon is of the same order as steel, standard steel fibers in SCC can be considered as rigid whereas long carbon fibers in Ordinary Rheology Concrete will be strongly deformed.

4. Random loose and dense packing of rigid fibers

The main difficulty when trying to apply the transition concept described in Section 1 to rigid fibers lies in the determination of the random loose packing or dense packing fractions of these specific inclusions. Whereas dense and maximum packing fractions for spheres are known and methods exist in the literature dealing with cementitious materials allowing for the measurement or even the prediction of dense and maximum packing fractions of mixtures of coarse aggregates [43], it is not the case for rigid fibers. It can first be noted that, as shown in Fig. 2, there is a strong variation in the apparent volume occupied by a given mass of fibers with the aspect ratio. Moreover, in the case of slender bodies, the difference between the maximum packing fraction and the dense packing fraction can be very high. It is indeed possible to imagine that, if an infinite amount of energy is brought to the system, the fibers will reorganize from a dense packing configuration similar to the one shown in Fig. 3(a) to the extreme maximum packing configuration shown in Fig. 3(b), for which the packing fraction reaches values higher than 80%.

We assess the random loose and dense packing fractions of fibers by measuring the apparent volumes Ω_{before} and Ω_{after} occupied by a mass M of fibers before and after vibration. The diameter and height of the testing recipient are larger than 5 times the length of the tested

Fig. 2. Apparent volumes occupied by identical mass of fibers in random packing for various fibers aspect ratio.

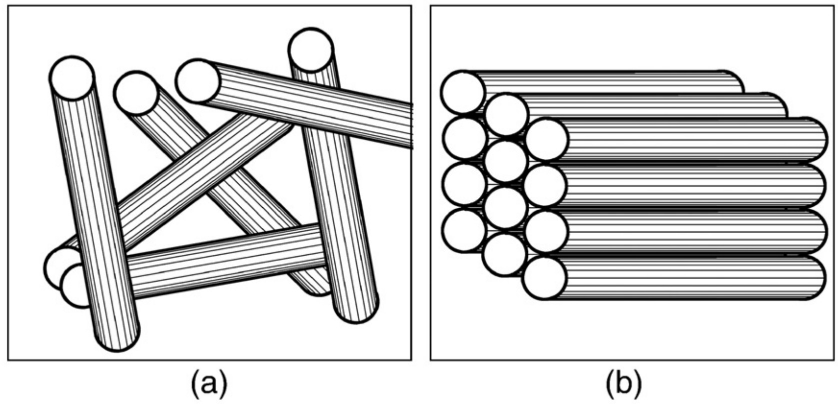

Fig. 3. Dense packing (a) and maximum packing (b) of rigid fibers.

fibers. As these measurements (especially Ω_{before}) strongly depend on minute changes in the filling process, three measurements were carried out for each type of fibers. We varied the vibration duration and intensity but were not able to measure any effects on the measured dense packing fraction as long as a vibration is applied. This can probably be explained by the fact that the network formed by the entangled fibers in dense packing is created very quickly and is very strong. If the density of the fibers is ρ_f, the random loose and dense packing fractions of the fibers ϕ_{fc} and ϕ_{fm} are then respectively calculated as the average values of $M/\Omega_{\text{before}}\rho_f$ and $M/\Omega_{\text{after}}\rho_f$.

Measurements were carried out for aspect ratio between 17 and 100 and are shown in Fig. 4. Both random loose packing and dense packing fractions rapidly decrease with increasing aspect ratio of the fibers and, as expected, when the aspect ratio has low values, dense packing fraction approaches 0.6, getting closer to the case of spherical inclusions.

Philipse [44] has shown that, in the case of high aspect ratio bodies (aspect ratio far higher than 1), it is possible to describe the dense packing fraction as:

$$\phi_{fm} = \alpha_m / r \quad (4)$$

or, in the case of random loose packing, as:

$$\phi_{fc} = \alpha_c / r \quad (5)$$

The values of α_m and α_c fitted using least squares method on our results in the range of high aspect ratios 50–100 are respectively 4 and 3.2 (Cf. Fig. 4). It can be noted that α_m is of the same order of magnitude as the value of 5.4 theoretically expected by Philipse [44] and that it is close to the value of order 4.5 which can be extrapolated

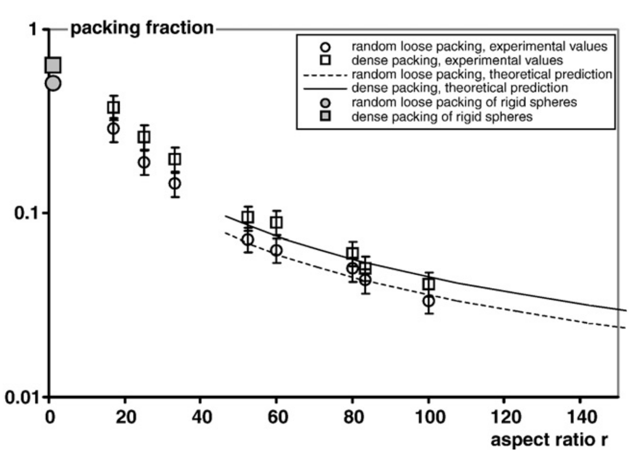

Fig. 4. Measured and predicted random loose packing and dense packing fractions as a function of the aspect ratio in the high aspect ratio range.

from the experimental work of Nardin and Papirer [45]. It can moreover be noted that, surprisingly, the ratio between random loose packing and dense packing fractions ϕ_{fc}/ϕ_{fm} is almost constant no matter the fiber aspect ratio in the studied range and is, as in the case of spherical inclusions, of the order of 0.8. Finally, it can be noted that Eqs. (4) and (5) cannot describe the results over the entire range of aspect ratio. This could have been expected as they are established assuming aspect ratio far higher than 1.

If the scaling described in the case of spherical inclusions in Section 1 is then applied here, this means that the behavior of a cementitious material containing fibers should scale on ϕ_f/ϕ_{fm} and therefore on $\phi_f r/\alpha_m$. As α_m does not depend on the fiber aspect ratio (at least for sufficiently high aspect ratio), this means that the behavior of the mixture should scale on $\phi_f r$ (the "fiber factor"). This is exactly what was obtained by most authors in the literature as described in the Introduction. It is thus not surprising that this factor is a very efficient way to qualitatively predict the evolution of the fluidity of the mixture as it is a direct indication of the number of contacts between fibers in the mixture and therefore of the strength of the fiber contact network in the material. Moreover, as it is not possible to pack fibers in a given mixture above the dense packing fraction $\phi_{fm} = \alpha_m/r$, this means that there should exist, as already described in the literature, a critical value of $\phi_f r$ above which fibers should tend to form *clumps* or *balls* and entrap air in the mixture. According to the results obtained here, as long as the fibers are the only inclusions in the cement paste, this critical value should be of the order of 4.

As a summary, as long as there are no inclusions other than fibers in the mixture, we can expect that, for fibers with high aspect ratio,

- if the fiber volume fraction is far lower than $\phi_{fc} = 3.2/r$, the influence of the fibers on the rheological behavior of the cementitious material should be low (Cf. Fig. 5(a)). As soon as ϕ_f gets close to $\phi_{fc} = 3.2/r$, the influence of the fibers on the rheological behavior starts to dominate all other effects.
- for fiber volume fractions between $\phi_{fc} = 3.2/r$ and $\phi_{fm} = 4/r$, the behavior of the cementitious material is strongly dominated by the contact network between the fibers (Cf. Fig. 5(b)). The material is far stiffer than its constitutive cement paste.
- for fiber volume fractions higher than $\phi_{fm} = 4/r$, the material should not be able to flow any more (Cf. Fig. 5(c)). Fibers should form balls and air should be entrained in the mixture.

5. Cement paste and fibers: yield stress measurements

5.1. Materials and experimental methods

The yield stresses of the tested suspensions were measured using a Haake viscotester VT550 and a Vane test procedure. The aspect ratio of

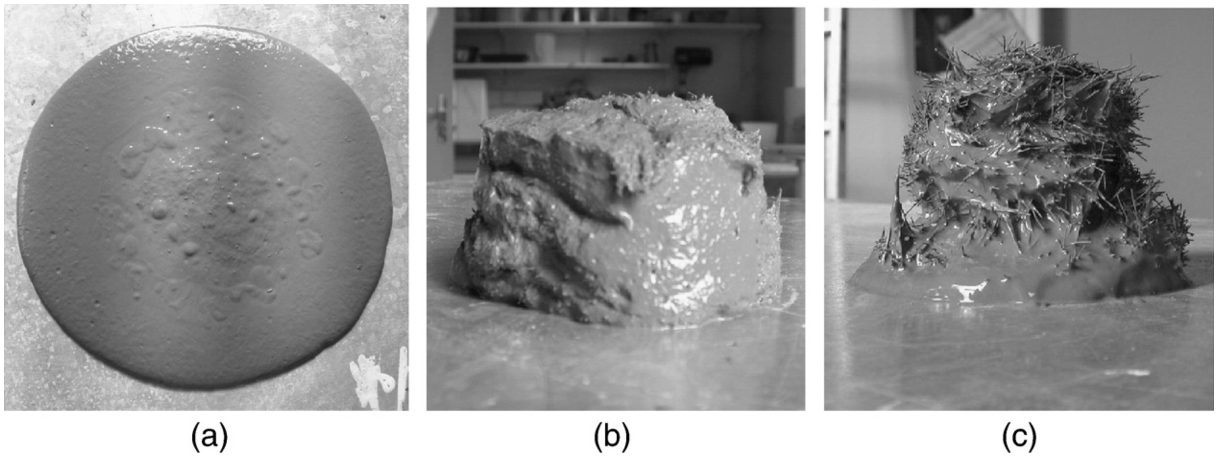

Fig. 5. Consistency of a cement paste (water to cement ratio 0.4) mixed with fibers with various aspect ratio. (a) $\phi_f r/\alpha_m = 0.18$; (b) $\phi_f r/\alpha_m = 0.83$; (c) $\phi_f r/\alpha_m = 1.02$.

the steel fibers tested in this section was between 33 and 80 (maximum length 10 mm). All dimensions of the fibers tested in this paper can be found in Table 1 and Fig. 6. The diameter of the Vane tool was 4 cm while the diameter of the bowl was 10 cm. The gap between the vane tool blades and the outer wall of the testing bowl was therefore 40 mm large (*i.e.* 5 times larger than the longest fibers). The height of material of the bowl was 10 cm. Both dynamic (or intrinsic) yield stress (just after mixing) and static (or apparent) yield stress (after rest) were measured to check the sensitivity of the mixture to resting time [46,47]. It can be kept in mind, that, in the rest of this paper, only the dynamic (or intrinsic) yield stress is studied. Both dynamic and static yield stresses after a one minute rest of the cement pastes tested here were between 25 and 30 Pa showing that the mixture studied was not strongly thixotropic. For each test, water and a water reducer of poly-carboxylate type (polymer to cement weight ratio of 1.3%) were mixed together and added to the cement powder (CEM I 52.5) before a 2 minute mixing phase (water to cement ratio equal to 0.4). The fibers were then added and the mixture was stirred by hand before being poured in the testing bowl. After a one minute resting time, the Vane test was carried out and typical measurements such as the one shown in Fig. 7 were obtained. As stated above, the fact that the cement paste without fibers does not show any peak can be linked with the fact that this mixture is not strongly thixotropic and that, during the one minute resting time, it does not have time to build a structure up. It can be noted here that a pre-shear phase before each test could not be carried out for this specific study as it would have strongly modified the orientation of the fibers in the bowl. However, as the resting time and the protocol were always the same, it can be considered that the effects of the structuration and of the thixotropy on the measurements can be neglected or at least do not affect the relative yield stress (*i.e.* the ratio between the yield stress of the cement paste containing fibers and the yield stress of the cement paste alone) which is used here. A new mixture was prepared for each test.

Table 1
Properties of the fibers tested in this paper.

Length (mm)	Thickness (mm)	Aspect ratio	Shape
3	0.175	17	Straight
5	0.2	25	Straight
5	0.15	33	Straight
10	0.2	50	Straight
42	0.8	52.5	Hooked end
55	1	55	Large end
15	0.25	60	Straight
20	0.25	80	Straight
25	0.3	83	Hooked end
30	0.3	100	Hooked end

It can be noted in Fig. 7 that, although the vane test result on the cement paste without fibers does not display a peak (*i.e.* the static yield stress after one minute rest is close to dynamic yield stress [46,47]), there exists a stress peak when fibers are added. This peak cannot be explained by thixotropy as the measurement was carried out at the same age and resting time as the reference cement paste. This peak is in fact due to the fiber orientation phenomenon. As soon as the material starts to flow, the fibers start to get a preferred orientation. This induced anisotropy reduces the energy needed to maintain the flow in the suspension and therefore reduces the measured stress level. We will limit our study in this paper to the peak value corresponding to the onset of flow and therefore to the yield stress of the isotropic material. What we call yield tress in the following will therefore be the value of the shear stress at the peak. However, as our material is not strongly thixotropic and the resting time is very short, the value at the peak will correspond to the dynamic yield stress of an isotropic mixture.

5.2. Experimental results

We plot in Fig. 8 the relative yield stress (*i.e.* ratio between the yield stress of the cement paste containing fibers and the yield stress of the cement paste without any fibers) as a function of the relative packing fraction $\phi_f r/\alpha_m$ with $\alpha_m = 4$ as measured in the previous section. The relative yield stress increases with increases in the relative packing fraction. It can be noted that the relative yield stress stay in the same order of magnitude (*i.e.* between 1 and 10) below the critical value of 0.8 (random loose packing fraction). As soon as the relative packing fraction reaches 0.6, data are far more scattered as the stress needed to initiate flow strongly depends on minute changes in the existing but not yet percolated network of contacts between fibers.

During these tests, the fibers sometimes tended to form balls. For example, for 14% fibers with aspect ratio 33, balls of fibers appeared and prevented any measurements of the behavior. This corresponds to a value of $\phi_f r/\alpha_m$ equal to 1.03, which is in agreement with the above theoretical frame. It has moreover to be noted that, for all materials, when $\phi_f r/\alpha_m$ becomes close to 0.9, hand mixing became particularly difficult and the rheometer torque was not sufficient to allow for any measurement.

6. Influence of the presence of other inclusions

In most applications, fibers are not the only inclusions in the cementitious mixture. They combine with sand and gravels in order to obtain the targeted properties. In this section, we propose to deal with these mixtures by simply adding the contribution of each type of inclusion to the contact network.

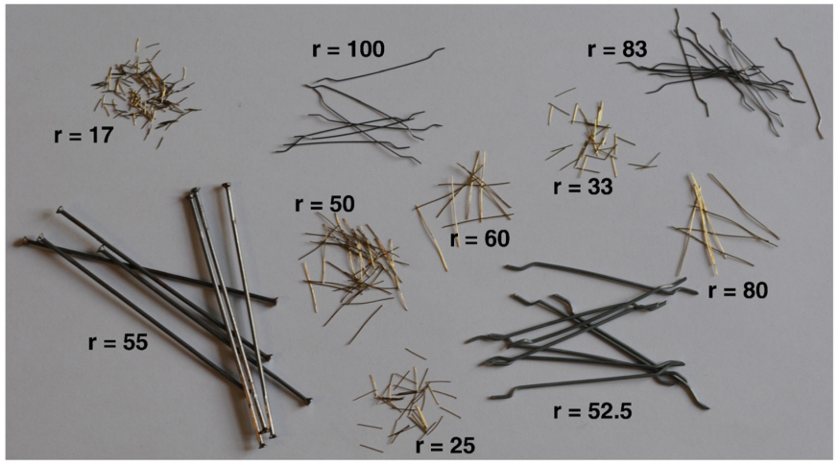

Fig. 6. Fibers tested in this paper (see Table 1 for details).

It has been demonstrated that fibers strongly affect the packing density of aggregates and vice versa [48]. Barthos and Hoy [49] noted that packing density is reduced with fiber addition in a slightly larger way with coarse aggregate than with sand, because “the sand is able to pack tightly around the fiber, whereas coarse aggregates are pushed apart by the fiber's presence”. This complex specific phenomenon illustrated in Fig. 9 cannot be quantitatively predicted without numerous experimental measurements allowing for the fitting of empirical coefficients [2,43]. As far as we know, it is not possible to take into account the presence of fibers in analytical model to predict the modified dense packing fraction of a granular skeleton made of various particles and to thereby predict the ideal proportions of small and large particles in a mix containing fibers. We have limited our approach here to materials containing only one size of particles or a sand fine enough to be considered as a part of the suspending paste such as fiber reinforced mortars or Ultra High Performance Fiber Reinforced Concretes (UHPFRC) which only contain fine sand particles.

We define the total relative volume fraction as the sum of the relative volume fraction of the fibers and the relative volume fraction of the granular skeleton $\phi_f r/4+\phi_s/\phi_m$ where ϕ_s and ϕ_m are respectively the volume fraction and the dense packing fraction of the sand. As, by doing this, we neglect the decrease of packing fraction of each individual specie due to wall effects or at the particle scale and, we probably underestimate the real global relative packing fraction of the inclusion mixture.

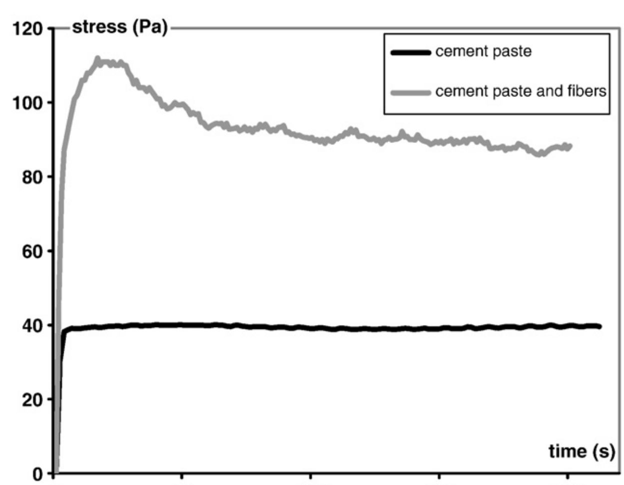

Fig. 7. Shear stress measured using a Vane test measurement as a function of time.

In this section, we examine yield stress measurements obtained from empirical tests like slump and slump flow tests using relations such as the ones given in [27–29]. We consider here that the flow duration of these empirical tests is not long enough to allow for fiber orientation. We did not consider in Fig. 10 the rich set of data obtained by Banfill et al. [26] as the fibers used in that work can be considered as flexible according to the rigidity criterion defined in Section 3. Moreover, we did not consider either the measurements obtained by Bui et al. in [23] or Kuder et al. [50] as these are affected by fiber orientation inside their rheometer.

We plot in Fig. 10 the relative yield stress (*i.e.* the ratio between the yield stress of the fiber reinforced material and the yield stress of the constitutive cement paste) as a function of the total relative packing fraction of inclusions (sand and fibers). We measured the dense packing fraction of our naturally rounded sand and obtained a value equal to 68%. This can be considered as a standard value according to [43]. The amount of sand in the mixtures was kept constant while the amount of fibers was varied. The sand contributed to the value of the relative packing fraction up to 0.65. It may be useful to point out that, because of expanded scale of the *Y*-axis, measured relative yield stresses for low relative packing fractions may seem to equal zero while they in fact equal 1.

We can see in Fig. 10 that it is possible to combine linearly the effects of both fibers and sand in order to identify the rapid increase in the yield stress of these mixtures around the critical volume fraction

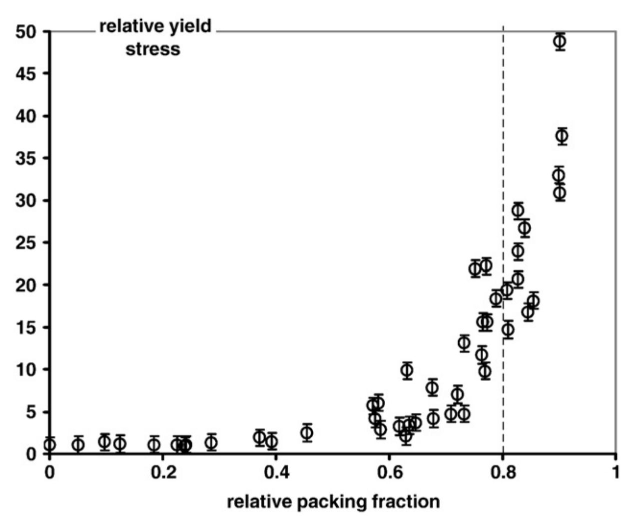

Fig. 8. Relative yield stress (i.e. ratio between the yield stress of the cement paste containing fibers and the yield stress of the cement paste without any fibers) as a function of the relative volume fraction $\phi_f r/\alpha_m$ with $\alpha_m = 4$. The dashed line corresponds to the critical random loose packing.

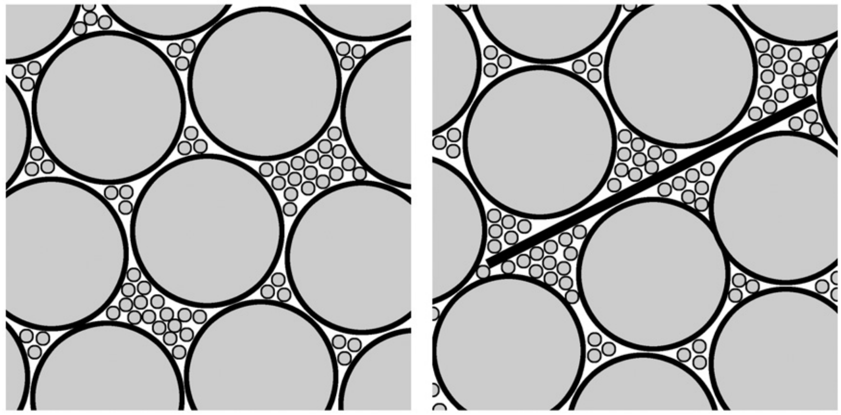

Fig. 9. Effect of a fiber on the packing of gravel and sand mixtures. In the above 2D dense packing example, the number of small grains needed to reach the densest packing is increased by roughly 20% whereas the number of large grains is decreased by roughly 10%.

at which all these inclusions combine in order to generate a strong direct contact network in the material. Below the random loose packing fraction, the fibers and inclusions only play a small role and the mixture behavior is very close to the cement paste behavior whereas, above the random loose packing fraction, the material yield stress increases by several orders of magnitude.

7. An additional mix design criterion for fiber reinforced mortars or UHPFRC

It is possible to extract from the above results a simple mix design criterion for UHPFRC. As the objective of mix design is to obtain the targeted fresh and hardened properties for the cheapest cost, it can be expected that an optimized mixture will contain as much sand as possible. The amount of sand will however be limited by the targeted workability of the material and strongly influenced by the amount and aspect ratio of the fibers.

If the total relative packing fraction defined above is higher than 100%, fibers should tend to form *clumps* or *balls* and entrap air in the mixture. The material will not be flowable. This means that the value of $\phi_f r/4+\phi_s/\phi_m$ should stay lower than 1. The maximum amount of fibers $(\phi_f)_{max}$ in the mixture to prevent this from happening is

$$(\phi_f)_{max} = \frac{400}{r}(1-\phi_S/\phi_m)\,(in\%) \qquad (6)$$

where r is the aspect ratio of the fibers, ϕ_s is the packing fraction of sand in the mixture and ϕ_m is the dense packing fraction of the sand (of order 65% for a rounded sand).

Eq. (6) captures the fact that it is possible to increase the fiber volume fraction in a given material by reducing the aspect ratio of the fiber, by reducing the packing fraction of granular skeleton or by choosing a sand displaying a higher dense packing fraction (*i.e.* naturally rounded sand instead of crushed sand for instance).

If the total relative packing fraction $\phi_f r/4+\phi_s/\phi_m$ is between 0.8 and 1, it can be considered that the mixture is optimized. If it is close to 1, it will probably be a firm mix as the contact network between fibers and aggregates will strongly diminish the ability to flow of the material. If it is close to 0.8, it will be possible to obtain a very fluid mix (even self compacting) by designing a fluid cement paste through the variation of the super-plasticizer dosage as the contribution of the direct contacts between aggregates and fibers to the consistency of the mix will be low.

Eq. (6) is now applied to the mix designs presented in [51–58] and which are claimed to be optimized through successive testing or analytical methods (*i.e.* these authors have introduced the highest amount of fibers while still getting a self compacting type mixture). The calculated total relative volume fractions of these mixes are plotted in Fig. 11. It can be seen that the above mix design criterion seems able to describe correctly the influence of both the fiber amount and shapes and the aggregate contribution to the yield stress of fiber reinforced concretes. It can be noted that, in the case of the mix design found in [58], three types of fibers are mixed together. In this specific

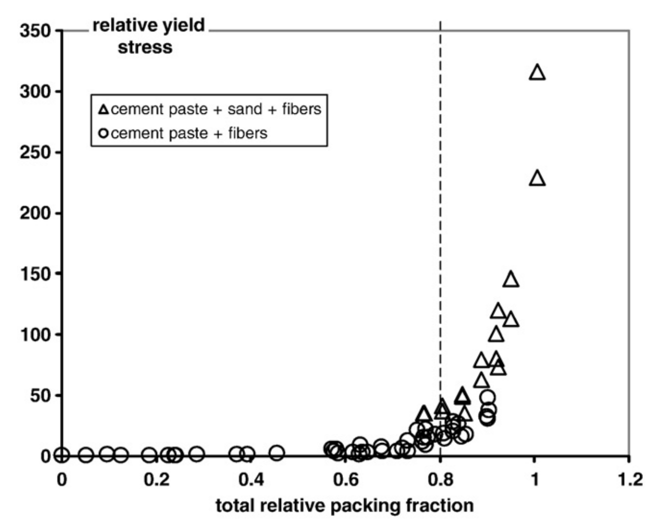

Fig. 10. Relative yield stress as a function of the total relative packing fraction. The dashed line corresponds to the theoretical random loose packing.

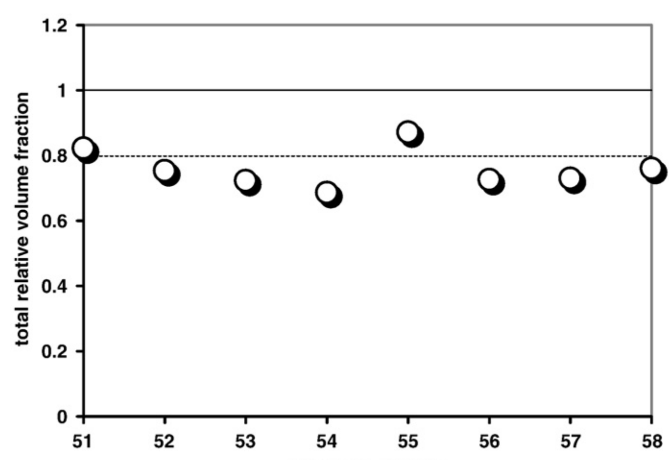

Fig. 11. Total relative packing fraction for the various mix designs in [51–58].

case, it is not possible to predict the dense packing fraction of the fibers using Eq. (4). We therefore measured it using the same fibers for the same proportions applying the procedure described in Section 4. The fiber mixture consisted in 27% of steel wool (measured dense packing fraction of 9%), 55% of short steel fibers (length 5 mm, diameter 0.15 mm, measured dense packing fraction of 14%) and 18% of long steel fibers (length 80 mm, diameter 0.25 mm, measured dense packing fraction of 5%). The measured dense packing fraction of this mixture of fibers was 15% showing that fibers, as any other inclusions can benefit from poly-dispersity.

8. Conclusions

In this paper, we have studied the effect of rigid straight fibers on the yield stress of cementitious materials. We have first derived from the physical phenomena involved in the case of spherical inclusions a simple model describing the contact network between rigid fibers inside the material. As soon as this contact network becomes percolated, the yield stress of the mixture increases by several orders of magnitude. We have then proposed a criterion allowing for the distinction between rigid and flexible fibers. We have then shown that a prediction of the critical fiber amount leading to a very strong increase of the yield stress of any cement paste, mortar or concrete could be derived from the proposed approach. This prediction assumes that the contribution of the aggregates and of the fibers to the contact network can simply be added. A simple and helpful mix design criterion for UHPFRC was finally proposed and applied to several mix proportions from the literature.

Acknowledgements

The authors wish to thank the French competitiveness cluster Advancity and the Region Île de France for their financial help.

References

[1] R.N. Swamy, Fiber reinforcement of cement and concrete, Mater. Struct. 8 (45) (1975) 235–254.
[2] S. Grünewald, Performance-based design of self-compacting fiber reinforced concrete, PhD-thesis, Section of Structural and Building Engineering, Delf University of Technology, Netherlands (2004).
[3] S. Grünewald, J.C. Walraven, Parameter-study on the influence of steel fibers and coarse aggregate content on the fresh properties of self-compacting concrete, Cem. Concr. Res. 31 (12) (2001) 1793–1798.
[4] H.B. Dhonde, Y.L. Mo, T.T.C. Hsu, J. Vogel, Fresh and hardened properties of self-consolidating fiber-reinforced concrete, ACI. Mater. J. 104-M54 (2007) 491–500.
[5] P. Rossi, Mechanical behaviour of metal-fibre reinforced concretes, Cem. Concr. Compos. 14 (1) (1992) 3–16.
[6] P. Soroushian, M.Z. Bayasi, Fiber-type effect on the performance of steel fiber reinforced concrete, ACI. Mater. J. 88 (2) (1991) 129–134.
[7] S.H. Li, S.P. Shah, Z. Li, T. Mura, Micromechanical analysis of multiple fracture and evaluation of debonding behavior for fiber-reinforced composites, Int. J. Solids Struct. 30 (11) (1993) 1429–1459.
[8] P. Soroushian, C.D. Lee, Distribution and orientation of fibers in steel fiber reinforced concrete, ACI. Mater. J. 87 (5) (1990) 433–439.
[9] Y. Akkaya, A. Peled, S.P. Shah, Parameters related to fiber length and processing in cementitious composites, Mater. Struct. 33 (2000) 515–524.
[10] B.P. Hughes, N.I. Fattuhi, Predicting the flexural strength of steel and polypropylene fiber-reinforced cement-based beams, Composites 8 (1) (1977) 57–61.
[11] B.P. Hughes, N.I. Fattuhi, Improving the toughness of high strength cement paste with fiber reinforcement, Composites 7 (3) (1976) 185–188.
[12] N. Banthia, J.F. Trottier, Deformed steel fiber-cementitious matrix bond under impact, Cem. Concr. Res. 21 (1) (1991) 158–168.
[13] N. Ozyurt, T.O. Mason, S.P. Shah, Non-destructive monitoring of fiber orientation using AC-IS: an industrial-scale application, Cem. Concr. Res. 36 (9) (2006) 1653–1660.
[14] R.J. Gray, C.D. Johnston, The effect of matrix composition on fiber/matrix interfacial bond shear strength in fiber-reinforced mortar, Cem. Concr. Res. 14 (2) (1984) 285–296.
[15] P. Rossi, P. Acker, Y. Malier, Effect of steel fibers at two different stages: the material and the structure, Mater. Struct. 20 (1987) 436–439.
[16] Y. Mohammadi, S.P. Singh, S.K. Kaushik, Properties of steel fibrous concrete containing mixed fibers in fresh and hardened state, Constr. Build. Mater. 22 (5) (2008) 956–965.
[17] B.P. Hughes, N.I. Fattuhi, The workability of steel-fiber-reinforced concrete, Mag. Concr. Res. 28 (9) (1976) 157–161.
[18] P. Rossi, N. Harrouche, Mix design and mechanical behaviour of some steel-fibre-reinforced concretes used in reinforced concrete structures, Mater. Struct. 23 (1990) 256–266.
[19] M.Z. Bayasi, P. Soroushian, Effect of steel fiber reinforcement on fresh mix properties of concrete, ACI. Mater. J. 89 (4) (1992) 369–374.
[20] C.D. Johnston, Proportioning, mixing and placement of fiber-reinforced cements and concretes, in: P.J.M. Bartos, D.L. Marrs, D.J. Cleland (Eds.), Production Methods and Workability of Concrete, RILEM Symposium, E&FN Spon, London, 1996, pp. 155–179.
[21] P. Groth, Fiber reinforced concrete — fracture mechanics methods applied on self-compacting concrete and energetically modified binders, PhD-thesis, Department of Civil and Mining Engineering, Lulea University of Technology (2004).
[22] P. Groth, D. Nemegeer, The use of steel fiber in self compacting concrete, in: A. Skarendahl, O. Petersson (Eds.), Self-compacting Concrete, RILEM Symposium Stockholm, RILEM publications, Cachan, 1999, pp. 497–508.
[23] V.K. Bui, M.R. Geiker, S.P. Shah, in: A.E. Naaman, H.W. Reinhardt (Eds.), Rheology of Fiber-reinforced Cementitious Materials, RILEM Publications (HPFRCC4, Michigan, 2003, pp. 221–231.
[24] Y. Ding, S. Liu, Y. Zhang, A. Thomas, The investigation on the workability of fiber cocktail reinforced self-compacting high performance concrete, Constr. Build. Mater. 22 (7) (2008) 1462–1470.
[25] L. Ferrara, Y.D. Park, S.P. Shah, A method for mix-design of fiber-reinforced self-compacting concrete, Cem. Concr. Res. 37 (6) (2007) 957–971.
[26] P.F.G. Banfill, G. Starrs, G. Derruau, W.J. McCarter, T.M. Chrisp, Rheology of low carbon fiber content reinforced cement mortar, Cem. Concr. Compos. 28 (9) (2006) 773–780.
[27] N. Roussel, Correlation between yield stress and slump: comparison between numerical simulations and concrete rheometer results, Mater. Struct. 39 (4) (2006) 501–509.
[28] N. Roussel, C. Stefani, R. Le Roy, From mini cone test to Abrams cone test: measurement of cement based materials yield stress using slump tests, Cem. Concr. Res. 35 (5) (2005) 817–822.
[29] N. Roussel, P. Coussot, “Fifty-cent rheometer” for yield stress measurements: from slump to spreading flow, J. Rheol. 49 (3) (2005) 705–718.
[30] R.N. Swamy, P.S. Mangat, Influence of fiber-aggregate interaction on some properties of steel fiber reinforced concrete, Mater. Struct. 7 (41) (1974) 307–314.
[31] A.G. Kooiman, Modeling steel fiber reinforced concrete for structural design, PhD thesis, Stevin Laboratory, Delft University of Technology (2000).
[32] I. Markovic, High-performance hybrid-fiber concrete — development and utilisation, PhD thesis, Department of Underground Infrastructure, Delft University of Technology (2006).
[33] P. Stähli, J.G.M. van Mier, Manufacturing, fiber anisotropy and fracture of hybrid fiber concrete, Eng. Fract. Mech. 74 (1–2) (2007) 223–242.
[34] F. Folgar, C.L. Tucker, Orientation behavior of fibers in concentrated suspensions, J. Reinf. Plast. Compos. 3 (1984) 98–119.
[35] R. Flatt, Towards a prediction of superplasticized concrete rheology, Mater. Struct. 27 (269) (2004) 289–300.
[36] Z. Toutou, N. Roussel, Multi scale experimental study of concrete rheology: from water scale to gravel scale, Mater. Struct. 39 (2) (2006) 189–199.
[37] J. Yammine, M. Chaouche, M. Guerinet, M. Moranville, N. Roussel, From ordinary rheology concrete to self compacting concrete: a transition between frictional and hydrodynamic interactions, Cem. Concr. Res. 38 (7) (2008) 890–896.
[38] I.M. Krieger, T.J. Dougherty, A mechanism for non-Newtonian flow in suspensions of rigid spheres, Trans. Soc. Rheol. 3 (1959) 137–152.
[39] M.R. Geiker, M. Brandl, L.N. Thrane, L.F. Nielsen, On the effect of coarse aggregates fraction and shape on the rheological properties of self compacting concrete, cement, Concrete and Aggregates 24 (1) (2002) 3–6.
[40] F. Mahaut, S. Mokeddem, X. Château, N. Roussel, G. Ovarlez, Effect of coarse particle volume fraction on the yield stress and thixotropy of cementitious materials, Cem. Concr. Res. 38 (11) (2008) 1276–1285.
[41] G.Y. Onoda, E. Liniger, Random loose packings of uniform spheres and the dilatancy onset, Phys. Rev. Lett. 64 (1990) 2727–2730.
[42] N. Roussel, A theoretical frame to study stability of fresh concrete, Mater. Struct. 39 (2006) 81–91.
[43] F. De Larrard, Concrete mixture proportioning, a scientific approach, in: Mindess, A. Bentur (Eds.), Modern Concrete Technology Series No 9, E & FN Spon, London, 1999.
[44] A.P. Philipse, The random contact equation and its implications for (Colloidal) rods in packings, suspensions, and anisotropic powders, Langmuir 12 (1996) 1127–1133.
[45] M. Nardin, E. Papirer, Contribution à l'etude des empilements au hasard de fibres et/ou de particules sphériques, Powder Tech. 44 (1985) 131–140.
[46] N. Roussel, A thixotropy model for fresh fluid concretes: theory, validation and applications, Cem. Concr. Res. 36 (10) (2006) 1797–1806.
[47] N. Roussel, Steady and transient flow behaviour of fresh cement pastes, Cem. Concr. Res. 35 (9) (2005) 1656–1664.
[48] P. Rossi, Steel fibre reinforced concrete (SFRC): an example of French research, ACI. Mater. J. 91 (3) (1994) 273–279.
[49] P.J.M. Barthos, C.W. Hoy, Interaction of particles in fibre reinforced concrete, in: P.J.M. Barthos, D.L. Marrs, D.J. Cleland (Eds.), Production Methods and Workability of Concrete, E&FN Spon, London, 1996, pp. 451–461.
[50] K.G. Kuder, N. Ozyurt, E.B. Mu, S.P. Shah, Rheology of fiber-reinforced cementitious materials, Cem. Concr. Res. 37 (2) (2007) 191–199.
[51] C. Magureanu, B. Heghes, O. Corbu, H. Szilagy, I. Sosa, Behaviour of high and ultra high performance fibre reinforced concrete, in: Proceedings of the 8th International Symposium on Utilization of High Strength and High Performance Concretes, Tokyo, 2008, pp. 353–356.
[52] Y. Sato, W. Pansuk, J.A. Den Uilj, J.C. Walraven, Shear capacity of high performance fibre reinforced concrete I-beams, in: Proceedings of the 8th International Symposium on Utilization of High Strength and High Performance Concretes, Tokyo, 2008, pp. 369–376.

[53] N. Sogabe, S. Yamanobe, T. Kono, Cyclic loading of high-seismic-performance RC piers with Ultra-High-Strength Fiber-Reinforced Concrete precast forms, in: Proceedings of the 8th International Symposium on Utilization of High Strength and High Performance Concretes, Tokyo, 2008, pp. 445–450.
[54] M. Sakurada, H. Ohyama, T. Mori, Application of High Strength Fiber Reinforced Mortar to prestressed concrete structures, in: Proceedings of the 8th International Symposium on Utilization of High Strength and High Performance Concretes, Tokyo, 2008, pp. 451–456.
[55] T. Mizutani, T. Yamada, N. Fujikura, H. Iwasaki, S. Tanaka, Development of manhole circular block using ultra high strength fiber reinforced concrete, in: Proceedings of the 8th International Symposium on Utilization of High Strength and High Performance Concretes, Tokyo, 2008, pp. 473–480.
[56] S.T. Kang, J.J. Park, J.H. Lee, S.W. Kim, The effect of the siliceous filler in ultra high strength concrete with steel fibers, in: Proceedings of the 8th International Symposium on Utilization of High Strength and High Performance Concretes, Tokyo, 2008, pp. 563–568.
[57] P. Rossi, Les bétons de fibres métalliques, Presses des Ponts et Chaussées, Paris, 1998.
[58] E. Parant, P. Rossi, C. Boulay, Fatigue behavior of a multi-scale cement composite, Cem. Concr. Res. 37 (2007) 264–269.